Electrochimica Acta 558 (2026) 148524

Contents lists available at ScienceDirect

Electrochimica Acta

journal homepage: www.journals.elsevier.com/electrochimica-acta

Inexpensive and rapid fabrication of paper-based electrochemical cells using a gold leaf and a toner laser printer

Michele Abate, Angela Cimmino, Gino Bontempelli, Nicolò Dossi *

Sustainable Analytical Instrumentation Laboratory (Sustain Lab), Department of Agrifood, Environmental and Animal Science, University of Udine, via Cotonificio 108, I-33100 Udine, Italy.

ARTICLE INFO

Keywords:
Paper-based electrochemical devices
Hydrophobic paper
Gold leaf electrodes
Toner-based analytical devices
Stripping voltammetry
Detection of heavy metals

ABSTRACT

This article presents a simple and innovative approach for the fabrication of flexible and low-cost planar electrochemical cells using paper-based gold leaf electrodes (PGLEs). This approach involves the use of a laser printer to selectively deposit toner onto a hydrophobic filter paper, which is then laminated with a gold leaf. The toner layer, which defines the design of the electrochemical circuit, acts as an adhesive and allows the gold to bond securely. The excess gold not adhering to the toner was gently removed using a cotton stick to create the working electrode, counter electrode, and reference electrode, with their contacts made with the thin layer of pure metal. The proposed approach takes advantage of readily available materials and common office tools that can be easily recovered even in low-resource settings. It allows the electrode geometry to be quickly modified but also to change the type of metal leaf adopted. In addition, the use of hydrophobic paper provides a viable alternative to plastic substrates for the fabrication of sustainable analytical devices capable of operating in both droplet and bulk mode. Furthermore, it must be also underlined that the functionality of the devices was not damaged during prolonged exposure to aqueous solutions. After optimization of the fabrication process, the electrochemical characterization of these cells was performed by using potassium hexacyanoferrate(II), hexamine ruthenium (III) chloride and dopamine as the prototype analytes. Voltammetric responses displayed a good inter-device reproducibility (5.4 %), thus confirming the effectiveness of this easy and fast assembling strategy. In these tests, the possibility of using a silver leaf to assemble PGLEs with Ag/AgCl reference electrodes was also assayed. Finally, PGLEs were tested for the quantification of lead and copper in tap water by square wave anodic stripping voltammetry, thus demonstrating that they displayed expected performances in various modes of operation. In particular, the proposed method presented a good linear range between 10 and 100 ppb and 2 and 100 ppb as well as low detection limits of 2.9 and 0.6 ppb for Pb^{2+} and Cu^{2+}, respectively. The dry construction process is an attractive option to other expensive, laborious, and time-consuming methods and does not require the use of solvents or post-production heat treatments and could be used to implement devices for flow-injection and microchip capillary electrophoresis analysis.

1. Introduction

The miniaturization of analytical devices can be considered one of the most effective strategies for achieving the objectives of Green Analytical Chemistry (GAC) as it combines portability and rapid analysis with low energy consumption and reduced waste, ensuring reliability and efficiency during analysis [1,2]. Its progress is linked to the development of microfluidic circuits, which are the basis of microreactors and separation microsystems, as they allow small quantities of reagents and eluents to be handled, minimizing the handling of chemicals and solvents. In recent years, there has been great interest in the study of innovative strategies for the construction of fluidic circuits, with particular attention to construction approaches based on widely available, low-cost technologies [3,4]. The literature reports numerous examples of microfluidic circuits made from flexible plastic or cellulose-based materials using common cutting plotters, lasers, or 3D printing [5–7]. Among the various technologies available, laser printing has been used to create fluidic circuits on paper and plastic, in which the fluidics consist of toner [8–10]. The same technology was used to create electrodes from CDs (Compact Discs), or PCBs (Printed Circuit Boards)

* Corresponding author.
E-mail address: nicolo.dossi@uniud.it (N. Dossi).

https://doi.org/10.1016/j.electacta.2026.148524
Received 23 December 2025; Received in revised form 20 February 2026; Accepted 23 February 2026
Available online 24 February 2026

that can be used in stand-alone mode or as detectors coupled with micro-separation systems [11,12]. In fact, electrochemical detection, in addition to being characterized by good sensitivity, is very well suited for integration into miniaturized systems, since electrochemical circuits can be made on various support materials, not only on glass and plastic but also on paper [13,14]. In paper-based electrochemical devices (PEDs), electrodes are frequently made of carbon-based materials such as graphene, carbon black, and carbon nanotubes because they are readily available, low-cost, and allow operation over wide potential ranges [15–17]. The conductive material can be deposited using techniques such as screen printing, pencil drawing, or laser scribing [18–20]. In most cases, filter papers or chromatography papers are used as the support, although hydrophobic paper could be a valid alternative to plastic materials to overcome the limitations due to the porous nature of cellulose fibers, which limits the migration of analytes to the electrode by convection and to form a well-defined electrode-electrolyte interface and improve mass transfer [21–23].

The assembling of electrodes based on metals, and especially noble metals, in paper-based devices remains an important goal. In fact, noble metals are widely used in electroanalysis due to their catalytic properties, often attributable to the ultra-thin metal oxide films that form spontaneously or are generated electrochemically at the electrode-solution interface [24,25]. Gold, in particular, is widely used owing to its high conductivity, its biocompatibility, and its high corrosion resistance [26,27]. Furthermore, thanks to the possibility of forming self-assembled monolayers (SAM) via thiol-gold bonds, biomolecules such as proteins and nucleic acids can be easily immobilized on the gold surface to create biosensors [28–30].

Although screen-printing techniques are still widely used, they have some limitations because ink and paste formulations often require the use of organic solvents and the deposition phase produces a lot of waste material [31,32].

Ink printing techniques (inkjet and aerosol printing) are very suitable for depositing inks containing metal particles or their precursors [33, 34]. Although these techniques allow direct writing of the conductive material onto the substrate and offer the possibility of quickly modifying the circuit design without having to use molds or masks, they require the production of inks whose chemical composition and rheological characteristics must be carefully formulated. Furthermore, after the deposition phase, thermal or laser-induced sintering processes often have to be carried out to make the printed traces conductive, thus making the entire process quite complex [35].

Techniques such as Chemical Vapor Deposition (CVD) and Physical Vapor Deposition (PVD) allow the formation of thin, high-purity metal films and the assembly of electrodes characterized by high electron transfer rates even on porous substrates such as paper [36,37]. However, this technique requires the use of complex and sophisticated equipment, which significantly affects the cost of paper- based electrochemical devices.

The possibility of obtaining electrodes made of pure metal is an important achievement because it avoids the presence on the electrode surface of substances that could compromise the activity of biomolecules or interfere with detection, especially in the determination of trace substances [38–40]. In fact, gold electrodes of different forms (solid as well as gold-film electrodes) have been used to detect heavy metals such as lead, copper, and mercury by stripping analysis [41–44].

This paper proposes a simple and innovative strategy for assembling miniaturized electrochemical cells consisting of three gold electrodes arranged in a planar configuration. With this approach, the gold traces are created through a process of hot lamination of gold leaf onto a hydrophobic paper substrate containing the electrochemical circuit design printed with a standard laser printer. The use of hydrophobic paper as the substrate allows for the creation of flexible and reusable electrochemical cells that can represent a sustainable and biodegradable alternative to those made with other techniques or on plastic materials. After a preliminary evaluation of their performance by hexacyanoferrate (II), hexamine ruthenium (III) chloride and dopamine as the prototype analytes, the capabilities of these paper-based gold leaf electrodes (PGLEs) were evaluated in the detection of Pb^{2+} and Cu^{2+} by stripping voltammetry, two heavy metal ions that can be present as contaminants in water and can be toxic to the human body with adverse effects on the immune, nervous, gastrointestinal, and reproductive systems.

2. Materials and methods

2.1. Reagents and instrumentation

Whatman® 1PS phase separator filter paper discs (Ø = 125 mm), potassium chloride, potassium hexacyanoferrate(II) trihydrate ($K_4[Fe(CN)_6]\cdot 3H_2O$), potassium hexacyanoferrate(III) ($K_3[Fe(CN)_6]$), hexamine ruthenium (III) chloride ($[Ru(NH_3)_6]Cl_3$), dopamine ($C_8H_{11}NO_2$), sodium hydrogen phosphate (Na_2HPO_4), sodium dihydrogen phosphate (NaH_2PO_4), nitric acid (HNO_3 65 %, SUPRAPUR®), 10.000 $mg\cdot L^{-1}$ Cu and Pb (Certipur®) solutions in HNO_3 2-3 % were purchased from Sigma-Aldrich (Sigma-Aldrich, Milano, I). Chloridric acid (HCl 37 %, AnalaR® NORMAPUR) and 28 multielements standard solution in HNO_3 5 % (Aristar®) from VWR International (Milano, I) were employed.

Deionized water obtained with a Purelab Flex 3 system (Elga, High Wycombe, UK) was used to prepare aqueous solutions. These consisted of 0.1 M phosphate buffers (pH=7), 0.1 M KCl, 0.5 M H_2SO_4 and 0.1 M HCl solutions. The standard solutions of $K_4[Fe(CN)_6]$, $K_3[Fe(CN)_6]$, $[Ru(NH_3)_6]Cl_3$, dopamine and those of the various metal ions were prepared in deionized water to obtain a final concentration of 10 mM and 100 $mg\cdot L^{-1}$, respectively. They were diluted when necessary to the desired concentration with the used electrolyte solution.

All glassware and plasticware used for preparing solutions and for measurements was thoroughly washed with soap and water and with a 1:1 v/v aqueous solution of concentrated nitric acid.

24-carat gold and silver leaves (AP Verona, Verona, IT), nail polish (Cosnova GmbH, DE), a laser printer (Canon C850i, Cernusco sul Naviglio, Milano, I) and a hot laminator (Hotseal H75, GBC, General Binding Corporation, Northbrook, IL, USA) were used to assemble paper-based gold leaf electrodes (PGLEs). The digital design of the electrochemical circuit to be printed was created using the Microsoft PowerPoint software (Redmond, WA, USA).

The composition of the toner (Canon, C-EXV 58) used in all experiments consisted of 79-80 % of the polyester-based resin and has been provided by the Material Safety Data Sheet (MSDS) of the manufacturer.

The real samples analyzed consisted of tap water taken from two different water networks. They were preliminarily acidified with HCl to obtain a final acid concentration of 0.1 M before being analyzed.

2.2. Construction of PGLEs

The PGLEs devices were assembled using an extremely simple and innovative procedure based on the use of common office tools. More specifically, a Whatman® filter paper disc was placed on a sheet of plain A4 paper, where it was fixed with a standard adhesive tape (Fig. 1 A). The A4 sheet was then inserted into the laser printer's input tray before starting the printing process, which transferred the digital design onto the paper (Fig. 1 B and C). Next, a gold leaf was placed on top of the Whatman® filter paper where the electrochemical circuit was printed (electrodes and their contacts made with the thin film of toner deposited during the printing process; Fig. 1 D). The A4 sheet of paper was then folded to cover the gold leaf and inserted into the hot laminator to allow the polymer material present in the toner to melt, thus adhering firmly to the gold leaf (Fig. 1 E). Once the hot lamination process was completed, the excess gold not adhering to the toner was gently removed using a cotton stick (Fig. 1 F). Finally, the individual PGLEs were separated from each other (Fig. 1 G) using a cutter and for each of them, the portion of the electrodes to be exposed to sample solutions was delimited by applying a thin layer of transparent nail polish, thus

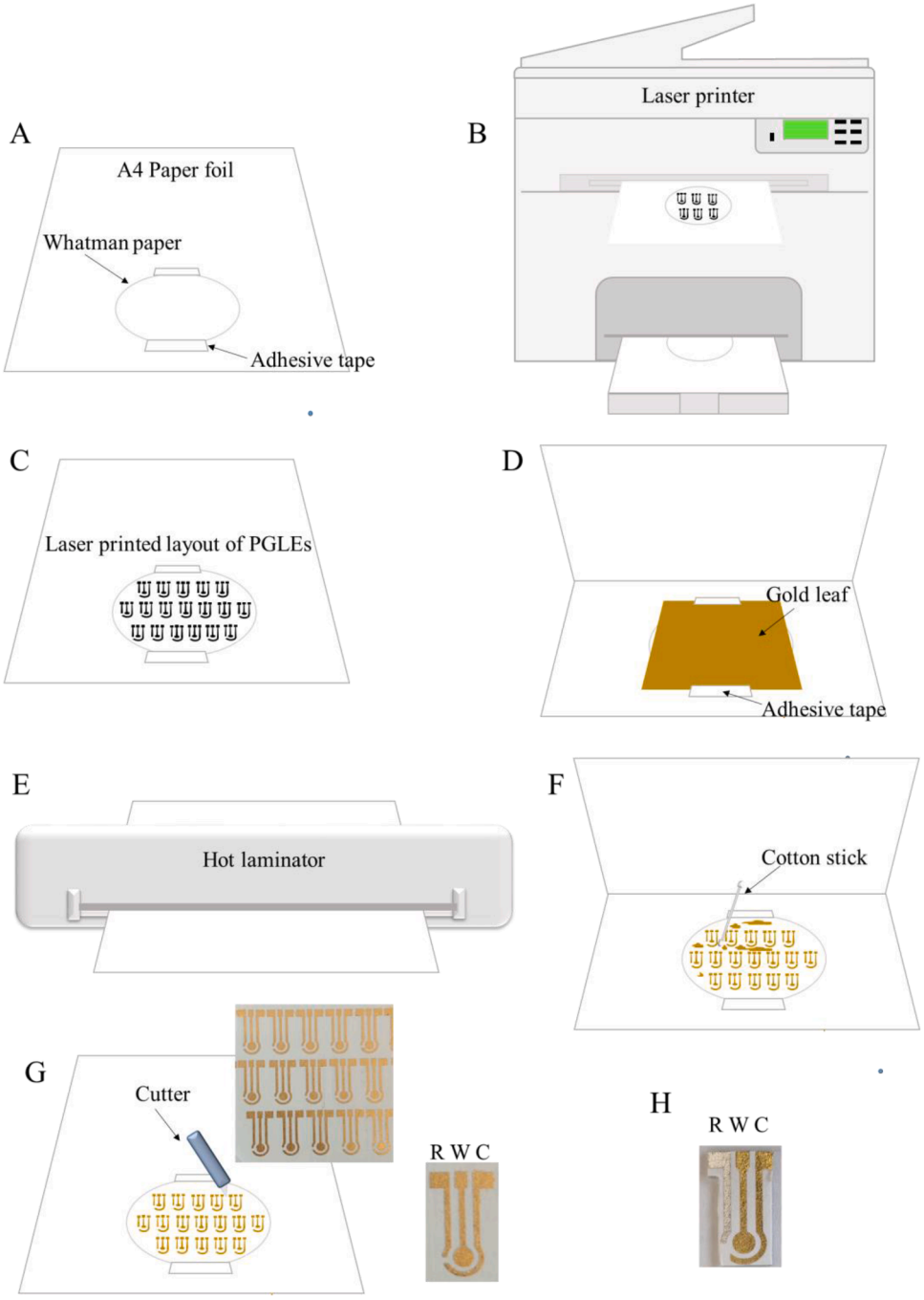

Figure 1. Scheme of the assembly procedure of the PGLEs and picture of the assembled cells.

obtaining working electrodes with a geometric area of 12.6 mm^2.

To construct PGLEs cells, where the Au pseudo-reference electrode was replaced by an Ag/AgCl reference electrode, the construction approach was slightly modified. This modification consisted of alternately placing strips of gold and silver leaf on the paper disc in correspondence with the toner traces for the counter-working electrode pair and the reference electrode, respectively. The PGLE obtained with this construction approach are shown in Fig. 1 H. The AgCl layer on the Ag surface was then electrogenerated by dipping the PGLEs in a 0.1 M KCl solution containing an Ag/AgCl, 3M KCl reference electrode and a platinum counter electrode by using the silver electrode as the working electrode at which a potential of 800 mV *vs*. Ag/AgCl, 3M KCl was applied for 30 s.

2.3. Electrochemical measurements

Conventional measurements were conducted with a Palmsens potentiostat (PalmSens, Houten, NL) driven by the relevant software and using an Ag/AgCl, 3M KCl reference electrode and a gold disc (Ø = 2 mm) (CH Instruments, Austin, TX, USA) as the working electrode.

PGLEs were used after a pre-treatment of their gold surface which was necessary to acquire repeatable signals and increase the sensitivity of measurements performed on the investigated analytes. To this end, PGLEs were preliminarily dipped for 5 s in a 10:1 v/v solution of H_2O: concentrated HNO_3. Also gold disc electrode was pre-treated by polishing its surface sequentially for 1 min with suspensions of 1, 0.3 and 0.05 μm of alumina powder. It was then immersed in stirred water to remove the remaining Al_2O_3 particles from the gold surface. The PGLEs

were used in two different operating modes. One was intended for performing measurements on controlled very small volume samples (90 µL) directly applied to the cell, which was placed in a horizontal position onto a planar surface (droplet mode). The second mode involved instead complete immersion of the cell, excluding contacts, in 50 mL glass beakers filled with 20 mL of an electrolyte solution containing known concentrations of the assayed analytes (bulk mode).

Cyclic voltammetric (CV) experiments performed using a 0.1 M KCl solution containing 1 mM of $K_4[Fe(CN)_6]$ were run in the potential window from -0.10 V to 0.60 V *vs.* an Ag/AgCl, 3M KCl reference electrode or from -0.20 V to 0.50 V *vs* the gold and Ag/AgCl pseudo-reference electrodes, respectively. In the case of voltammetric tests conducted with 1 mM $[Ru(NH_3)_6]Cl_3$ in 0.1 M KCl and dopamine in phosphate buffer, the potential windows ranged from 0.25 to -0.5 and from -0.1 to 0.6 *vs.* an Ag/AgCl, 3M KCl, respectively.

Square wave anodic stripping voltammetric (SWASV) measurements were performed as follows: i) conditioning at 0.5 V for 30 s ($E_{cond.}$); ii) accumulation at -0.4 V performed for 120 s under continuous stirring ($E_{dep.}$); iii) 10 s equilibration in quiet solution ($t_{eq.}$); iv) SWV stripping from -0.4 to 0.5 V at 11 Hz frequency (f), step potential 3 mV ($E_{step.}$) and amplitude 28 mV ($E_{amp.}$). Prior to conduct investigations involving cathodic processes, the oxygen present in the solutions was removed by degassing with a nitrogen flow for 15 min under stirring. Electrochemical conditioning of the surface of PLEGs was found essential to get a good baseline and a stable voltammetric stripping response of metals. With this aim, fresh electrodes for stripping measurements were preliminarily conditioned by applying 5 potential cycles in the range between 0 and 0.7 V with a scan rate of 50 $mV{\cdot}s^{-1}$ in a 0.1 M HCl solution.

The electrochemical impedance spectroscopy (EIS) measurements were carried out using a potentiostat/galvanostat AUTOLAB (model PGSTAT 302N Metrohm, Utrecht, NL) equipped with an impedance modulus. EIS data were obtained using an open circuit potential (0.22 V vs. Ag/AgCl, 3M KCl) in the presence of 1 mM of $K_4[Fe(CN)_6]$/ $K_3[Fe(CN)_6]$ redox probes in 0.1 M KCl, applying a potential of 10 mV AC over a frequency range from 100 KHz to 0.10 Hz under static conditions. Nyquist plots were generated and fitted using the equivalent Randles circuit to determine the charge transfer resistance (R_{ct}) using the NOVA 2.1.8 software.

2.4. ICP-OES measurements

The element amounts determined by SWASV were compared with those found by an Inductively Coupled Plasma Optical Emission Spectrometer (ICP-OES), model ICP-OES 5800 (Agilent Technologies Italia, Cernusco sul Naviglio, Milano, I), operating at RF power 1.20 kW and using argon gas (99.998 %, White Martins Praxair, Araucária, Brazil) in plasma generation (12.05 $L{\cdot}min^{-1}$), auxiliary (1.01 $L{\cdot}min^{-1}$) and nebulizer (0.70 $L{\cdot}min^{-1}$). A concentric nebulizer combined with a single pass nebulizer chamber was used in the sample introduction system. The analytical signal measurements were performed in the axial viewing mode at the following wavelengths (nm): Pb 220.4 and Cu 327.4. A multi-element standard solution in HNO_3 5 % (VWR International, Milano, I) was used for instrumental calibration conducted for all the analysed elements in the range 0-100 $\mu g{\cdot}L^{-1}$.

3. Results and discussion

3.1. Characterization of PGLEs in bulk mode experiments

Preliminary investigations were carried out to evaluate the electrochemical behavior of the assembled PGLEs using the methodology described in the experimental section. For this purpose, potassium hexacyanoferrate(II), dissolved at a concentration of 1 mM in a 0.1 M KCl solution, was used as the redox probe for understanding the direct interaction between the electrode and the redox species. The tests were initially conducted in a conventional cell using a volume of 20 mL with the aim of verifying the cell resistance to swelling caused by contact with water. The PGLEs were dipped in the solution, avoiding wetting the part with the electrical contacts. A platinum electrode as counter electrode and an Ag/AgCl, 3M KCl reference electrode, in order to have a stable reference, were also inserted into the same cell. In these preliminary experiments, only the working electrode of the PGLE device was connected to the potentiostat circuit. This configuration allowed the insertion of a gold disc working electrode into the same cell, which was used to perform comparative measurements after its mechanical cleaning with alumina.

As it can be seen from Fig. 2 (dotted black line), in the range considered between -0.1 and 0.6 V, the background electrolyte did not show any signal attributable to interference from the gold layer exposed to the solution or to transfers from the toner.

However, tests carried out on a series of 10 newly produced PGLEs showed that in some cases the voltammetric profile of $K_4[Fe(CN)_6]$ was characterized by poor reversibility, a clear sign of inefficient electron transfer to the electrode surface (Fig. 2, green line). On the contrary, the signal produced by the mechanically cleaned disc electrode always showed a well-defined profile characterized by a ΔEp equal to 70 mV, typical of a quasi-Nernstian behavior (Fig. 2, red line).

These results confirmed the importance of cleaning the electrode surface to remove any organic impurity present on the surface and the oxides that normally form when gold is exposed to air.

In fact, upon exposure to a non-cleanroom laboratory environment, the gold surface is subject to numerous ambient contaminants, affecting the binding kinetics of biomolecules in addition to electrochemical effects [45]. This aspect can be particularly critical when the electrode material consists of inks or thin metal films and mechanical cleaning could be difficult.

Based on these results, the PGLEs were subjected to a surface cleaning treatment consisting of immersion for 5 s in a solution of H_2O and concentrated HNO_3 in a ratio of 10:1 (v/v) in order to remove impurities present on the surface due to the handling of the devices during their preparation phase and any potential residues remaining from the production of the gold leaves.

Obviously, the use of a material such as paper excludes the possibility of using overly concentrated acid solutions.

As it can be seen from Fig. 2 (blue line), the voltammetric profile recorded after surface cleaning on $K_4[Fe(CN)_6]$ as a redox probe with a scan rate of 50 $mV{\cdot}s^{-1}$ was characterized by a well-defined profile and a peak-to-peak separation ΔEp equal to 75 mV, quite similar to that obtained on a disc electrode after mechanical cleaning. It is important to note that in the case of the disc electrode, no substantial changes in the voltammetric profile of potassium hexacyanoferrate(II) were observed when the same treatment was performed after the mechanical cleaning cycle.

This result, together with the ratio between the anodic and cathodic peak currents very close to 1, underlines the quasi-reversible behavior of the process at PGLEs, thus highlighting their good electrochemical properties.

Additionally, an analysis of the characteristics at the electrode/solution surface was conducted through EIS experiments using equimolar solutions of $K_4[Fe(CN)_6]$ and $K_3[Fe(CN)_6]$. As shown in Fig. 2 (inset), EIS results were consistent with those of CV tests conducted at PGLEs in that the charge transfer resistance R_{ct} decreased after the pre-treatment, indicating an improvement of the electron transfer.

Inter-electrode reproducibility was verified using different cells (n=20) made in different days and it was found to be 5.4 and 5.2 % for both the peak current (both anodic and cathodic) and the ΔEp. Furthermore, tests carried out by varying the scan rate in the range between 5 and 200 $mV{\cdot}s^{-1}$ verified that peak current increased linearly with the square root of the scan rate ($y(\mu A)=2.1804x\ (mV{\cdot}s^{-1})^{1/2}-0.8588$, $R^2=0.998$).

Tafel plots were drawn from data of the rising part of the current-voltage curves recorded at 5 $mV{\cdot}s^{-1}$ for potassium hexacyanoferrate(II)

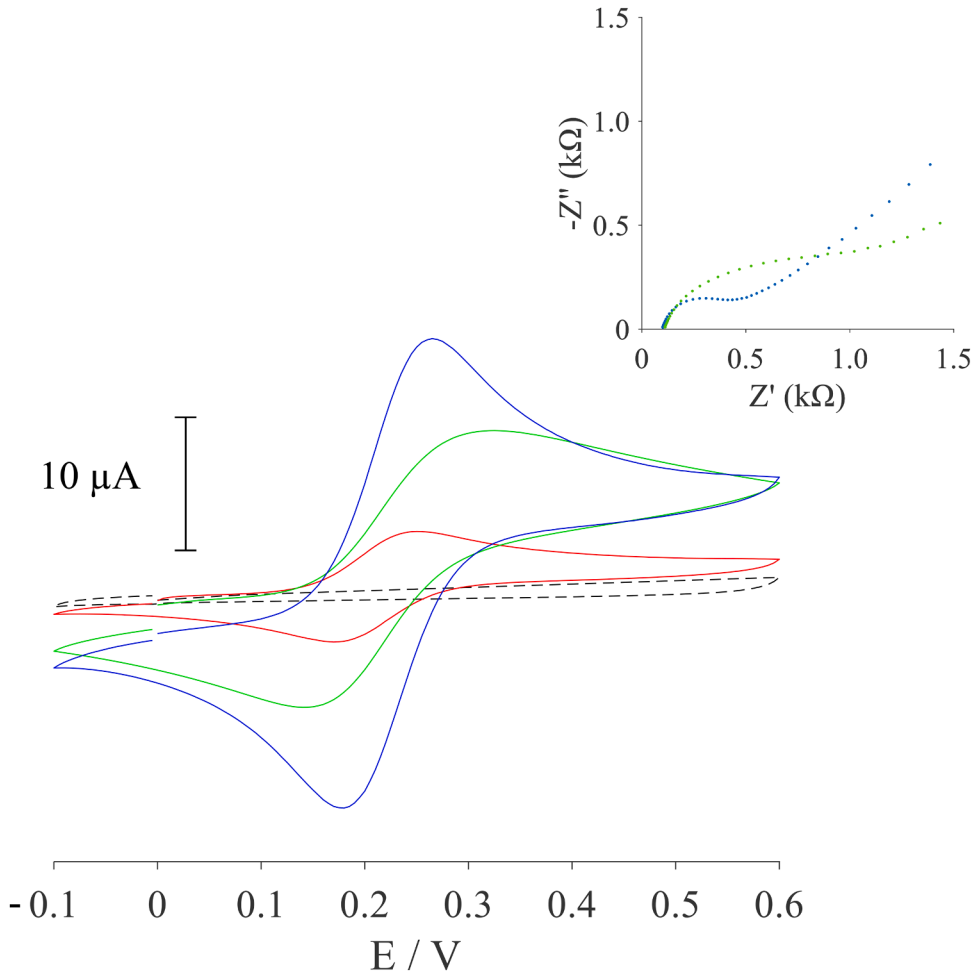

Figure 2. Cyclic voltammograms of 1 mM of $K_4[Fe(CN)_6]$ in 0.1 M KCl recorded at a mechanically polished gold disc electrode (red line) and at fresh (green line) or pre-treated (blue line) PGLE *vs.* an external Ag/AgCl, 3M KCl. Scan rate 50 mV·s^{-1}. Inset: EIS Nyquist plots recorded in the presence of 1 mM of both $K_4[Fe(CN)_6]$ and $K_3[Fe(CN)_6]$ at bare (green line) and pre-treated (blue line) PGLEs .

obtaining slopes of 0.122 V·dec^{-1} and 0.118 V·dec^{-1} for gold discs and PGLEs, respectively. From these plots, also the corresponding values of the transfer coefficients α 0.52 and 0.49 were obtained.

Subsequently, cyclic voltammograms in the range between 5 and 200 mV·s^{-1} at pre-treated PGLEs were recorded on the electrochemical probe $[Ru(NH_3)_6]^{3+}$ by using different scan rates, to gain information on the occurrence of the electron transfer and how electron transfer occurs through the electrolyte. As shown in Figure 3, well defined profiles were recorded with a peak-to-peak separation (ΔEp equal to 74 mV at a scan rate of 50 mV·s^{-1}), very similar to that found at a disc electrode after mechanical cleaning (71 mV). Also in these tests the peak current increased linearly with the square root of the scan rate (plot equation: y (µA) = -3.398x (mV·s^{-1})$^{1/2}$-2.154; R^2=0.998).

These trends, typical of diffusion-controlled electrochemical processes, allows the slope of the corresponding regression plot to be associated with the electrochemical area of the electrode using the Randles-Sevcik equation [46–49] for quasi-reversible electrochemical processes as reported in the Supplementary materials.

Scan rate studies were also exploited to determine the heterogeneous electron transfer rate constant (k^0) following the Nicholson approach [50]. k^0 values of (14.9 ± 0.8)·10^{-3} cm· s^{-1} and (24.5 ± 2.0)·10^{-3} cm· s^{-1} were found at PGLEs, whereas k^0 values of (15.9 ± 0.6)·10^{-3} cm· s^{-1} and (25.7 ± 1.8)·10^{-3} cm· s^{-1} at gold disc electrodes were found when experiments were conducted with $K_4[Fe(CN)_6]$ and $[Ru(NH_3)_6]Cl_3$, respectively. Also, comparing Figs. 2 and 3, it becomes clear that no charged functional group is present on the electrode surface after pre-treatment.

The electrochemical behavior of PGLEs was also evaluated in a 0.5 M H_2SO_4 solution by performing 20 cycles in the potential range from 0.0 to 1.6 V *vs.* Ag/AgCl, 3M KCl in order to assess the crystallinity of the gold surface [51].

As it can be observed in Fig. 3 (inset), the first CV exhibited a broad peak centred at 1.35 V and distinct peaks starting to evolve with multiple overlapping oxidation peaks, in agreement with what was observed for the gold disc electrode under the same conditions. They were due to the different exposed crystal planes, typical of polycrystalline structures, which appear as a result of surface restructuring by electrochemical cycling in H_2SO_4. The most characteristic peak is the reduction peak observed at -0.87 V, which is a quite symmetric well-shaped peak corresponding to the reduction of gold oxides [52,53].

Tests performed using dopamine as a model of non-ionic organic compound confirmed the effectiveness of PGLEs. In fact, as it can be seen in Fig. 4, which shows the voltammetric profiles recorded using solutions with increasing concentrations of this analyte dissolved in phosphate buffer pH=7, well-defined anodic peaks were recorded, whose height was linearly dependent on the analyte concentration. Peak-to-peak separation (ΔEp) equal to 325 mV at a scan rate of 50 mV·s^{-1} was found.

The calibration plots constructed using the heights of the anodic peaks were found to be y(µA)=0.0277 C(µM) + 0.438 (R^2=0.998) and the detection limit, calculated as 3σ/S (where σ is the standard deviation calculated on the background noise and S is the sensitivity determined

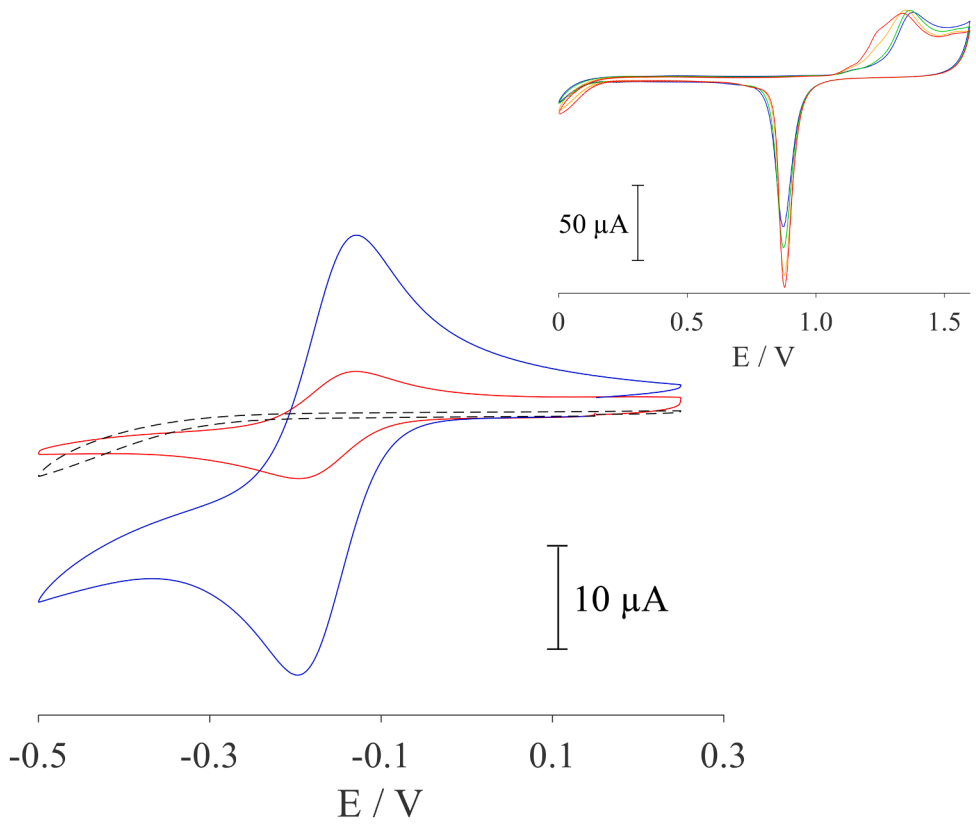

Figure 3. Cyclic voltammograms of 1 mM of $[Ru(NH_3)_6]Cl_3$ in 0.1 M KCl recorded at a mechanically polished gold disc electrode (red line) or pre-treated (blue line) PGLE *vs.* an external Ag/AgCl, 3M KCl. Scan rate 50 $mV \cdot s^{-1}$. Inset: Repeated cyclic voltammograms recorded at a PGLE in 0.5 M H_2SO_4 at scan rate of 50 $mV \cdot s^{-1}$.

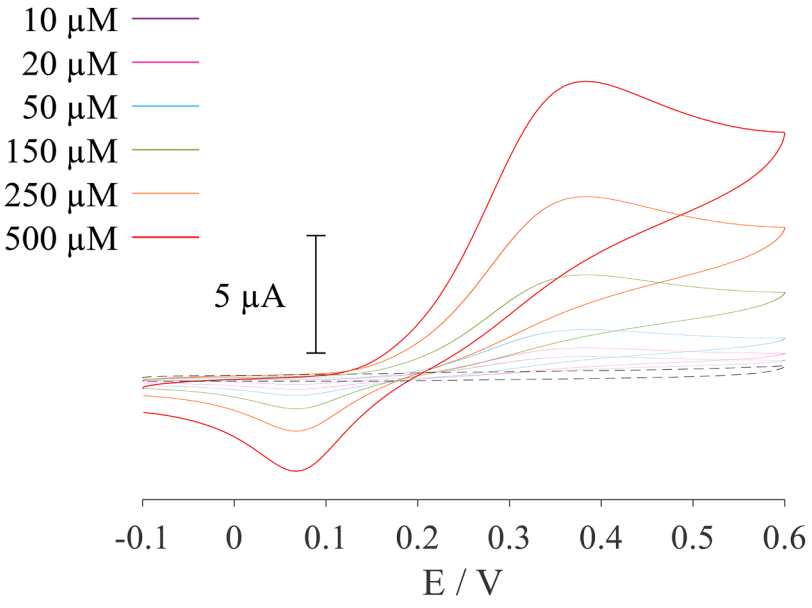

Figure 4. Cyclic voltammograms of dopamine at different concentrations in 0.1 M phosphate buffer recorded at pre-treated PGLE *vs.* an external Ag/AgCl, 3M KCl. Scan rate 50 $mV \cdot s^{-1}$.

from the calibration curve), was found to be 2.5 µM.

After these tests, the resistance of the assembled devices to the swelling caused by water was evaluated by conducting a series of voltammetric scans for the potassium hexacyanoferrate(II) every 30 min for 3 h. The good repeatability of the results obtained (RSD % equal to 3.1 and 3.5 for peak current and ΔEp, respectively) showed that in the time interval considered, which was abundantly longer than that required to construct a calibration plot and to perform the analysis of many samples, the stay in water was not going to alter the performance of PGLEs.

On the other hand, toners appear an attractive material due to the hydrophobic properties of PET that make it a material suitable for creating barriers for paper-based devices and microfluidic channels, due to the excellent adhesion to paper and various membranes or foils [54–56]. In addition, this result confirmed the validity of the choice of

hydrophobic paper and the possibility of using this material as an alternative to plastic materials.

3.2. Characterization of PGLEs in droplet mode experiments

After verification of the validity of the production process and of the cleaning procedure and the evaluation of the proper operation of the PGLEs in bulk mode experiments, the possibility of using them also in the droplet mode was evaluated. This mode of operation makes it possible to work with sample amounts in the microliter range [57], ensuring a reduction in the used reagents, waste production, and increased operator safety.

Before proceeding with voltammetric tests, PGLEs were subjected also in this case to a pre-treatment with aqueous nitric acid solution. The tests were first performed by connecting only the working electrode and counter electrode to the potentiostat circuit and using an external Ag/AgCl, 3M KCl reference electrode. It was placed vertically with respect to the plane of the electrochemical device by dipping the porous septum in the drop consisting of the analyzed solution. Importantly, due to the hydrophobic nature of the paper, when a drop of water-based solutions was placed on the surface of the PGLEs it immediately achieved a spherical shape, due to the surface tension causing water molecules to pull inward rather than spread out and to the poor adhesion at the interface.

Fig. 5 (black line) reports the voltammetric profile of $K_4[Fe(CN)_6]$ in 0.1 M KCl recorded at the scan rate of 50 mV·s^{-1} which shows that the change in the operating mode did not go to interfere with the behavior of the paper-based device, as it was expected. In fact, the signal obtained was characterized by a well-defined profile, good reversibility and an $E_{1/2}$, calculated as the mean of Ep_a and Ep_c equal to 0.220 ± 0.007 V.

The same tests using the gold electrode as a pseudo-reference (Fig. 5, blue line) showed a potential shift of 0.105± 0.005 V of the $E_{1/2}$, but this potential tended to move slowly toward more anodic potentials by repeating the scans.

Finally, PGLEs in which the reference electrode consisted of a silver leaf were tested. Before these tests the Ag surface was anodically covered by an AgCl layer as described in the experimental section. As it can be seen from Fig. 5 (red line), the voltammetric profiles of the ferrocyanide/ferricyanide pair recorded using these PGLEs were characterized by an average potential between Ep_a and Ep_c equal to 0.133 ± 0.005 V that was similar to that measured with the gold pseudo-reference electrode and more cathodic than that found using Ag/AgCl, 3M KCl. These results are in agreement with those expected, considering that for quasireversible and reversible processes, the half-wave potentials $E_{1/2}$ are coincident with the corresponding formal standard potentials E°' [58]. In particular, for the redox system in 0.1 M KCl, the determined value of 0.133 ± 0.005 V was quite close to the expected value (0.128 ± 0.005 V) obtained by subtracting from the value of the standard potential for the hexacyanoferrate(II)/(III) system at pH=7 (E°' = 0.41 V [58]), i.e. the theoretical value of E of Ag/AgCl, 0.1 M KCl equal to 0.281 V.

Similar voltammetric profiles were obtained using an external Ag/AgCl reference electrode equipped with a porous septum and filled with a KCl solution at a concentration of 0.1 M. These results confirmed the possibility of constructing PGLEs devices equipped with stable reference electrodes.

Finally, in order to evaluate the elastic behavior of the devices, their electrochemical performance was tested after 5 bending cycles (5 times at 120°). The CV profiles were then compared with those obtained before the bending tests, and no significant differences were observed.

Therefore, it could be concluded that the structure of the electrodes after bending did not cause any alteration that could affect the electrochemical results.

3.3. Detection of heavy metals by square wave anodic stripping voltammetry

In order to use PGLEs for an application of great importance in food and environmental fields and of interest for public health, their analytical performance has been verified for the determination of metal ions and in particular for the quantification of copper and lead ions in drinking water. In fact, high heavy metal concentrations in wastewater, such as copper and lead, are extremely dangerous to human health and have drawn a lot of attention in the field of environmental management. Lead is frequently found in paints, batteries, alloys, and fuel and is considered among the most hazardous elements [59]. Copper plays instead a vital role as an essential trace element. However, its excessive intake contributes to a spectrum of serious health issues [60].

Before proceeding with the analysis of the real samples, the performance of PGLEs was verified using the standard solutions prepared following the procedure described in section 2.1.

The tests were carried out using the bulk mode owing to the need to eliminate the presence of oxygen to avoid its interference in the stripping measurements. Square-wave anodic stripping voltammetry was used for the determination of Pb^{2+} and Cu^{2+} in a concentration range of some μg·L^{-1} using the following operational conditions: E_{cond}: +0.5 V for 30 s, E_{dep}: -0.4 V for 120 s, t_{eq}: 10 s; E_{amp}: 28 mV, E_{step}: 3 mV, f: 11 Hz suggested in the literature [61].

Again, after their assembly and before their use, PGLEs were treated

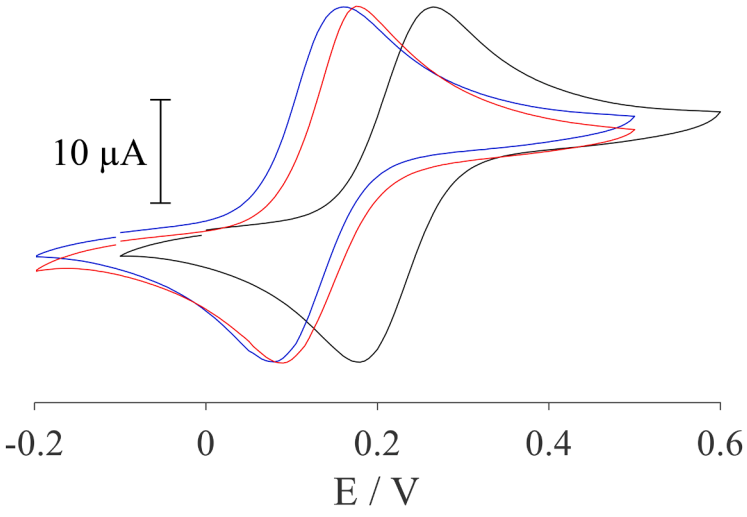

Figure 5. Cyclic voltammograms of 1 mM of $K_4[Fe(CN)_6]$ in 0.1 M KCl recorded at a PGLE *vs.* an external Ag/AgCl, 3M KCl (black line), internal Au (blue line) or Ag/AgCl (red line) reference electrode. Scan rate 50 mV·s^{-1}.

with H_2O and HNO_3-based solutions (10:1, v/v).

Measurements were made using hydrochloric acid as the supporting electrolyte not only because it is widely used for electrochemical detection of heavy metals by stripping voltammetry, but also because it ensures a constant concentration of chloride ions in the supporting electrolyte medium [61–64]. This is particularly important when an Ag/AgCl-based pseudo-reference electrode is used. In agreement with the literature, the concentration of HCl present in the electrolyte was 0.1 M [61]. The PGLE was placed into the cell and the electrochemical conditioning of the surface was performed to obtain a proper baseline and a stable response [65]. It was performed by applying 5 cycles by cyclic voltammetry (CV), using the following conditions: medium 0.1 M HCl, potential range between 0.0 and 0.7 V and scan rate 50 $mV \cdot s^{-1}$ [66].

Preliminary tests using a solution containing Pb(II) and Cu(II) at a concentration of 50 $\mu g \cdot L^{-1}$ showed that under these experimental conditions it was possible to obtain narrow peaks with good shape with peak maxima located at -0.11 and 0.34 V, respectively.

Intra-device repeatability was verified by making 10 repetitive measurements of the same solution using the same experimental parameters, and the relative standard deviation calculated on peak height was found to be 4.2 %. Inter-device reproducibility was also evaluated using 10 different PGLEs assembled at different times, which was found to be satisfactory with an RSD % = 5.9, calculated on the height of the voltammetric peaks.

Finally, the optimized parameters were subsequently adopted to analyze Pb and Cu solutions at increasing concentrations between 10 and 100 $\mu g \cdot L^{-1}$ and 2 and 100 $\mu g \cdot L^{-1}$ for Pb and Cu, respectively. As shown in Fig. 6, the measurements generated well-defined anodic peaks whose height was linearly dependent on the analyte concentration.

Importantly, the same results were obtained when the Ag/AgCl pseudo-reference electrode was used even if, to account for the potential shift due to the change in chloride ion concentration, the instrumental parameters were changed, shifting all potentials by a value of 90 mV in the cathodic direction. A displacement of the peak potentials equal to about 100 mV was observed.

Then, the calibration plots were constructed using the heights of the anodic peaks and they were found to be $y(\mu A)=0.00945\ C_{Pb}(\mu g \cdot L^{-1}) + 2.274$ ($R^2=0.99$) and $y(\mu A)=0.2769\ C_{Cu}(\mu g \cdot L^{-1}) + 3.403$ ($R^2=0.99$) for Pb and Cu, respectively. The detection limit, calculated as $3\sigma/S$ was found to be 2.9 and 0.6 $\mu g \cdot L^{-1}$ for Pb and Cu, respectively.

Similar results in terms of electrochemical background profile and peak shape and potentials of Cu^{2+} and Pb^{2+} species were obtained using the gold disc electrode although, due to its smaller electrode surface area, the recorded signals were lower (Fig. 6, inset).

3.4. Analysis of real samples

After the evaluation of the performance of PGLEs with synthetic samples, real samples were analyzed. They consisted of drinking water from two different water networks (samples A and B). An aliquot of sample B was left for 24 h inside a metal bottle to assess the possible release of metals over time and was here referred as sample C. In all cases, before analyses, all samples were acidified with HCl to obtain an acid concentration of 0.1 M.

From the analyses conducted on one of the samples (A), it was found to contain high copper concentrations, so that it was preliminarily subjected to a 1:3 v/v dilution with deionized water before its acidification with HCl.

Moreover, to further evaluate the quantification step, voltammetric measurements were performed by adding controlled Pb and Cu concentrations of 20 or 50 $\mu g \cdot L^{-1}$ on both the sample A, diluted 1:3 v/v with deionized water, and on sample C. The difference between the height of the anodic peak recorded following the addition of the two analytes and that of the peak before the addition was related to the calibration plot constructed with the standard metal ion solutions. The value obtained from this ratio made it possible to estimate that the recovery under these conditions was 97±5 %.

The concentrations of Pb and Cu, expressed as µg of metal per L of all samples (ppb) are reported in Table 1. The same samples were also analyzed by the ICP-OES technique in order to compare the results obtained with the laboratory-built device with those obtained by serving traditional benchtop instrumentation.

ICP-OES performed on the same samples revealed comparable contents, demonstrating that the device thus assembled can be successfully

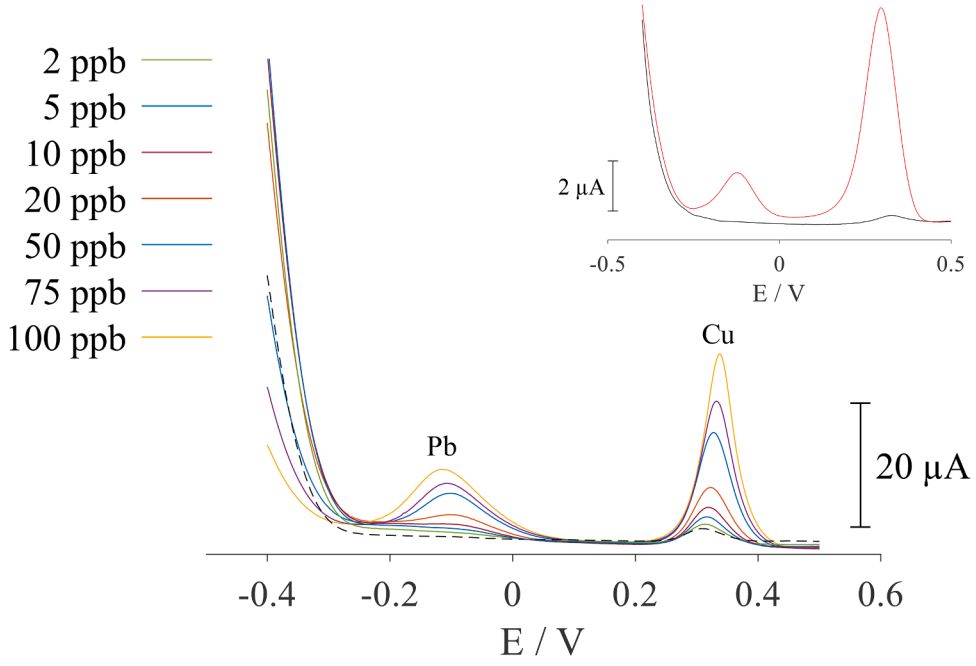

Figure 6. SWASV scans recorded at a PGLE in HCl 0.1M (dotted line) to which increasing concentrations of Pb(II) and Cu(II) were added. SWASV scans recorded at a gold disc in HCl 0.1 M (black line) to which 100 $\mu g \cdot L^{-1}$ of Pb(II) and Cu(II) were added (inset). SWASV conditions: $E_{cond.}$ +0.5 V for 30 s, $E_{dep.}$: -0.4 V for 120 s, $t_{eq.}$: 10 s; $E_{amp.}$: 28mV, $E_{step.}$: 3mV, f: 11 Hz.

Table 1
Lead and copper concentrations ($\mu g \cdot L^{-1}$) obtained by SWASV using PGLE and by ICP-OES for real water samples.

Sample	Spiked		Found by PGLE		Found by ICP-OES	
	C_{Pb} ($\mu g \cdot L^{-1}$)	C_{Cu} ($\mu g \cdot L^{-1}$)	C_{Pb} ($\mu g \cdot L^{-1}$)	C_{Cu} ($\mu g \cdot L^{-1}$)	C_{Pb} ($\mu g \cdot L^{-1}$)	C_{Cu} ($\mu g \cdot L^{-1}$)
A:H_2O (1:3, v/v)	0	0	n.d	27 ±1.1	n.d	30 ±0.03
A:H_2O (1:3, v/v)	20	20	18 ±0.7	48 ±1.8	19 ±0.02	51 ±0.05
A:H_2O (1:3, v/v)	50	50	47 ±1.8	79 ±3.1	50 ±0.05	82 ±0.08
B	0	0	n.d.	6±0.2	n.d	7±0.01
C	0	0	n.d	6±0.2	n.d	7±0.01
C	20	20	22 ±0.8	25 ±0.9	21 ±0.02	27 ±0.03
C	50	50	53 ±2.1	58 ±2.3	51±0.0	57 ±0.06

n.d.= not detectable

used for metal measurements. It must be underlined that in sample C (water left in the metal bottle), no release of metals from the container was detected.

4. Conclusions

The approach here proposed enables the construction of electroanalytical devices that allow analyses to be performed in compliance with the fundamental principles of Green Analytical Chemistry (GAC) and Democratic Analytical Chemistry (DAC). In fact, they can be made with simple construction technologies, readily available and biodegradable materials and allow very small sample amounts to be analyzed, while minimizing the handling of chemicals by operators and the production of waste.

Their construction requires only computers equipped with a graphic software and an office laser printer. Some accessories easily found, such as a laminator and a simple cutter, are also required. It allows both the shape and size of the electrodes to be changed easily and quickly by simply modifying the digital design, which can be designed with any other graphic software.

Compared with other construction approaches that rely on the use of inks, the method here proposed allows for conductive traces consisting of pure gold free of dopants that could contribute to the heterogeneity of the electrodes and interfere during detection at ppb levels. Results confirmed that gold leaves allow the fabrication of electrodes with high-quality crystalline surfaces, without requiring the use of complex instrumentation and clean rooms, making them favorable for applications requiring stable, homogeneous and self-assembled performance, as for biosensor development.

The method allows many devices to be produced in a short time at very low cost (about 0.35 euros/PGLE). In addition, the excess gold resulting from the fabrication process and in the form of fragments can be recovered and reused to make electrochemical devices by taking advantage of other existing approaches in which the electrochemical circuit design consists of simple adhesive tape [67].

Furthermore, thanks to the availability on the market of other metals in the form of thin foil, such as copper, silver, palladium, and platinum, the same approach can be used to produce a wider range of PGLEs, significantly expanding the range of applications.

CRediT authorship contribution statement

Michele Abate: Writing – original draft, Methodology, Investigation, Formal analysis, Data curation. **Angela Cimmino:** Investigation, Formal analysis. **Gino Bontempelli:** Writing – review & editing. **Nicolò Dossi:** Writing – review & editing, Writing – original draft, Supervision, Methodology, Funding acquisition, Conceptualization.

Declaration of competing interest

The authors declare that they have no known competing financial interests or personal relationships that could have appeared to influence the work reported in this paper.

Supplementary materials

Supplementary material associated with this article can be found, in the online version, at doi:10.1016/j.electacta.2026.148524.

Data availability

Data will be made available on request.

References

[1] A. Agrawal, R. Keçili, F. Ghorbani-Bidkorbeh, C.M. Hussain, Green miniaturized technologies in analytical and bioanalytical chemistry, TrAC-Trends Anal. Chem 143 (2021) 116383, https://doi.org/10.1016/j.trac.2021.116383.
[2] E. Psillakis, Towards sustainable analytical chemistry, TrAC-Trends Anal. Chem 191 (2025) 118371, https://doi.org/10.1016/j.trac.2025.118371.
[3] S. Smith, M. Sypabekova, S. Kim, Towards sustainable analytical chemistry, Biosensors 14 (2024) 249, https://doi.org/10.3390/bios14050249.
[4] J. Ho Shin, S. Choi, Open-source and do-it-yourself microfluidics, Sens. Actuator B-Chem 347 (2021) 130624, https://doi.org/10.1016/j.snb.2021.130624.
[5] D.I. Walsh, D.S. Kong, Shashi K. Murthy, P.A. Carr, Enabling microfluidics: from clean rooms to makerspaces, Trends Biotechnol 35 (2017) 383–392, https://doi.org/10.1016/j.tibtech.2017.01.001.
[6] Z. Li, N. Haridas, S. Kaaliveetil, Y.-H. Cheng, C. Chande, V. Perez, A.K. Miri, S. Basuray, Low-cost rapid prototyping for microfluidics using Parafilm®-based microchannels for low resource settings, Sens. Actuator B-Chem 404 (2024) 135212, https://doi.org/10.1016/j.snb.2023.135212.
[7] M.A. Selemani, K. Cenhrang, S. Azibere, M. Singhateh, R.S. Martin, 3D printed microfluidic devices with electrodes for electrochemical analysis, Anal. Methods 16 (2024) 6941, https://doi.org/10.1039/d4ay01701c.
[8] J.S. Ng, M. Hashimoto, Fabrication of paper microfluidic devices using a toner laser printer, RSC Adv 10 (2020) 29797, https://doi.org/10.1039/d0ra04301j.
[9] C.L. Do Lago, H.D. Torres da Silva, C.A. Neves, J.G. Alves Brito-Neto, J.A.F. da Silva, A dry process for production of microfluidic devices based on the lamination of laser-printed polyester films, Anal. Chem 75 (2023) 3853–3858, https://doi.org/10.1021/ac034437b.
[10] E.F.M. Gabriel, G.F. Duarte Junior, P.d.T. Garcia, D.P. De Jesus, W.K.T. Coltro, Polyester-toner electrophoresis microchips with improved analytical performance and extended lifetime, Electrophoresis 33 (2012) 2660–2667, https://doi.org/10.1002/elps.201200009.
[11] D. Lowinsohn, E.M. Richter, L. Angnes, M. Bertotti, Disposable gold electrodes with reproducible area using recordable CDs and toner masks, Electroanalysis 18 (2006) 89–94, https://doi.org/10.1002/elan.200503385.
[12] W.K.T. Coltro, D.P. De Jesus, J.A.F. da Silva, C.L. Do Lago, E. Carrilho, Toner and paper-based fabrication techniques for microfluidic applications, Electrophoresis 31 (2010) 2487–2498, https://doi.org/10.1002/elps.201000063.
[13] B.M.D.C. Costa, S. Griveau, F. d'Orlye, F. Bedioui, J.A.F. da Silva, A. Varenne, Microchip electrophoresis and electrochemical detection: a review on a growing synergistic implementation, Electrochim. Acta 391 (2021) 138928, https://doi.org/10.1016/j.electacta.2021.138928.
[14] W. Dungchai, O. Chailapakul, C.S. Henry, Electrochemical detection for paper-based microfluidics, Anal. Chem 81 (2009) 5821–5826, https://doi.org/10.1021/ac9007573.
[15] H. Barich, O. Voet, N. Sleegers, J. Schram, N.Felipe Montiel, V. Beltran, G. Nuyts, K. De Wael, Selecting optimal carbon inks for fabricating high-performance screen-printed electrodes for diverse electroanalytical applications, J. Electroanal. Chem 971 (2024) 118585, https://doi.org/10.1016/j.jelechem.2024.118585.
[16] E. Noviana, C.P. McCord, K.M. Clark, I. Jang, C.S. Henry, Electrochemical paper-based devices: sensing approaches and progress toward practical applications, Lab Chip 20 (2020) 9–34, https://doi.org/10.1039/C9LC00903E.
[17] S. Michalkiewicz, A. Skorupa, M. Jakubczyk, Carbon materials in electroanalysis of preservatives: a review, Materials 14 (2021) 7630, https://doi.org/10.3390/ma14247630.
[18] N. Dossi, F. Terzi, E. Piccin, R. Toniolo, G. Bontempelli, Rapid prototyping of sensors and conductive elements by day-to-day writing tools and emerging manufacturing technologies, Electroanalysis 28 (2016) 250–264, https://doi.org/10.1002/elan.201500361.
[19] W.A. Ameku, M. Negahdary, I.S. Lima, B.G. Santos, T.G. Oliveira, T.R.L.C. Paixão, L. Angnes, Laser-scribed graphene-based electrochemical sensors: a review, Chemosensors 10 (2022) 505, https://doi.org/10.3390/chemosensors10120505.
[20] C.M.G. Ribeiro, L.V. da Silva, J.D. Gonçalves, L.D. Pinho, M.E.M. Sanches, R.F. de Barros, M.O. Salles, Advances in carbon-based electrodes: characterization of

screen-printed and laser-induced graphene techniques, J. Solid State Electrochem (2025), https://doi.org/10.1007/s10008-025-06400-3.
[21] A.C. Glavan, D.C. Christodouleas, B. Mosadegh, H.D. Yu, B.S. Smith, J. Lessing, M. T. Fernández-Abedul, G.M. Whitesides, Folding analytical devices for electrochemical ELISA in hydrophobic R^H paper, Anal. Chem 86 (2014) 11999–12007, https://doi.org/10.1021/ac5020782.
[22] T. Yun, Y. Tao, Q. Li, Y. Cheng, J. Lu, Y. Lv, J. Du, H. Wang, Superhydrophobic modification of cellulosic paper-based materials: fabrication, properties, and versatile applications, Carbohydr. Polym 305 (2023) 120570, https://doi.org/10.1016/j.carbpol.2023.120570.
[23] R.B. Channon, M.P. Nguyen, A.G. Scorzelli, E.M. Henry, J. Volckens, D.S. Dandy, C. S. Henry, Rapid flow in multilayer microfluidic paper-based analytical devices, Lab Chip 18 (2018) 793–802, https://doi.org/10.1039/C7LC01300K.
[24] M. Avramov-Ivić, V. Jovanović, G. Vlajnić, J. Popić, The electrocatalytic properties of the oxides of noble metals in the electro-oxidation of some organic molecules, J. Electroanal. Chem 423 (1997) 119–124, https://doi.org/10.1016/S0022-0728(96)04787-0.
[25] P.J. Obeid, N. Sari-Chmayssem, P. Yammine, D. Homsi, H. El-Nakat, Z. Matar, S. Hamieh, D. Koumeir, A. Chmayssem, Designs and materials of electrodes for electrochemical sensors, ChemElectroChem 12 (2025) e202500230, https://doi.org/10.1002/celc.202500230.
[26] K. Partanen, Y. Pei, P. Hillen, M. Hassan, K. McEleney, G. Schatte, S.J. Payne, R. Oleschuka, Z. She, Investigating electrochemical deposition of gold on commercial off-the-shelf 3-D printing materials towards developing sensing applications, RSC Adv 12 (2022) 33440, https://doi.org/10.1039/d2ra05455h.
[27] M.K. Puglia, P.K. Bowen, Cyclic voltammetry study of noble metals and their alloys for use in implantable electrodes, ACS Omega 7 (2022) 34200–34212, https://doi.org/10.1021/acsomega.2c03563.
[28] D.D. Liana, B. Raguse, L. Wieczorek, G.R. Baxter, K. Chuah, J.J. Gooding, E. Chow, Sintered gold nanoparticles as an electrode material for paper-based electrochemical sensors, RSC Adv 3 (2013) 8683, https://doi.org/10.1039/c3ra00102d.
[29] J.K. Lee, H.N. Suh, H.-b. Park, H.J. Kim, S.H. Kim, Double step electrochemical etching for reuse of gold screen printed electrode, ACS Omega 10 (2025) 49260–49271, https://doi.org/10.1021/acsomega.5c02911.
[30] I. Podunavac, M. Kukkar, V. Léguillier, F. Rizzotto, Z. Pavlovic, L. Janjušević, V. Costach, V. Radonic, J. Vidic, Low-cost goldleaf electrode as a platform for Escherichia coli immunodetection, Talanta 259 (2023) 124557, https://doi.org/10.1016/j.talanta.2023.124557.
[31] E. Maiorano, S. Gianvittorio, M. Lanzi, D. Tonelli, H. Pick, A. Lesch, Print-light-synthesis of gold thin film electrodes for electrochemical sensing, Adv. Mater. Technol 8 (2023) 2202039, https://doi.org/10.1002/admt.202202039.
[32] T. Kant, K. Shrivas, K. Tapadia, R. Devi, V. Ganesan, M.K. Deb, Inkjet-printed paper-based electrochemical sensor with gold nano-ink for detection of glucose in blood serum, New J. Chem 45 (2021) 8297, https://doi.org/10.1039/d1nj00771h.
[33] A. Määttänena, U. Vanamob, P. Ihalainena, P. Pulkkinenc, H. Tenhuc, J. Bobackab, J. Peltonena, A low-cost paper-based inkjet-printed platform for electrochemical analyses, Sens. Actuator B-Chem 177 (2013) 153–162, https://doi.org/10.1016/j.snb.2012.10.113.
[34] Y. Sui, C.A. Zorman, Review-Inkjet printing of metal structures for electrochemical sensor applications, J. Electrochem. Soc 167 (2020) 037571, https://doi.org/10.1149/1945-7111/ab721f.
[35] M. Zamani, C.M. Klapperich, A.L. Furst, Recent advances in gold electrode fabrication for low-resource setting biosensing, Lab Chip 23 (2023) 1410, https://doi.org/10.1039/d2lc00552b.
[36] A. Balapure, S. Fande, P. Nair, N.R. Gurram, S.K. Dubey, S. Chattopadhyay, S. Goel, Physical vapor deposition of gold electrodes on flexible and inflexible substrates for electrochemical applications, Chem. Eng. J 522 (2025) 167343, https://doi.org/10.1016/j.cej.2025.167343.
[37] L.Y. Shiroma, M. Santhiago, A.L. Gobbi, L.T. Kubota, Separation and electrochemical detection of paracetamol and 4-aminophenol in a paper-based microfluidic device, Anal. Chim. Acta 725 (2012) 44–50, https://doi.org/10.1016/j.aca.2012.03.011.
[38] D. García García, L. Espinosa Garcia, E.O. Madrigal-Santillán, J. A. Morales-González, E. Madrigal-Bujaidar, I. Álvarez-González, P. Damian-Matsumura, J.E. Jiménez-Salazar, N. Batina, L.F. Garcia-Melo, Impact of cleaning procedures on screen-printed gold electrodes performance for mutation detection, J. Appl. Electrochem 55 (2005) 1937–1946, https://doi.org/10.1007/s10800-025-02271-8.
[39] T.J. Rabbow, N. Junker, C. Kretzschmar, M. Schneider, A. Michaelis, Electrochemically induced degradation of screen-printed gold thick films, J. Ceram. Sci. Technol 3 (2012) 199–210, https://doi.org/10.4416/JCST2012-00023.
[40] G. Paimard, E. Ghasali, M. Baeza, Screen-printed electrodes: fabrication, modification, and biosensing applications, Chemosensors 11 (2023) 113, https://doi.org/10.3390/chemosensors11020113.
[41] K.C. Honeychurch, Cheap and disposable gold and silver electrodes: trends in the application of compact discs and digital versatile discs for electroanalytical chemistry, TrAC-Trends Anal. Chem 93 (2017) 51e66, https://doi.org/10.1016/j.trac.2017.04.013.
[42] A. Giacomino, A. Ruo Redda, S. Squadrone, M. Rizzi, M.C. Abete, C. La Gioia, R. Toniolo, O. Abollino, M. Malandrino, Anodic stripping voltammetry with gold electrodes as an alternative method for the routine determination of mercury in fish. Comparison with spectroscopic approaches, Food Chem 221 (2017) 737–745, https://doi.org/10.1016/j.foodchem.2016.11.111.
[43] S. Laschi, G. Bagni, I. Palchetti, M. Mascini, As(III) voltammetric detection by means of disposable screen-printed gold electrochemical sensors, Anal. Lett 40 (2007) 3002–3013, https://doi.org/10.1080/00032710701645703.
[44] P. Prasertying, N. Jantawong, T. Sonsa-ard, T. Wongpakdee, N. Khoonrueng, S. Buking, D. Nacapricha, Gold leaf electrochemical sensors: applications and nanostructure modification, Analyst 146 (2021) 1579, https://doi.org/10.1039/d0an02455d.
[45] L.M. Fischer, M. Tenje, A.R. Heiskanen, N. Masuda, J. Castillo, A. Bentien, J. Émneus, M.H. Jakobsen, A. Boisen, Gold cleaning methods for electrochemical detection applications, Microelectron. Eng 86 (2009) 1282–1285, https://doi.org/10.1016/j.mee.2008.11.045.
[46] R.D. Crapnell, E. Sigley, R.J. Williams, T. Brine, A. Garcia-Miranda Ferrari, C. Kalinke, B.C. Janegitz, J.A. Bonacin, C.E. Banks, Circular economy electrochemistry: recycling old mixed material additively manufactured sensors into new electroanalytical sensing platforms, ACS Sustain. Chem. Eng 11 (2023) 9183–9193, https://doi.org/10.1021/acssuschemeng.3c02052.
[47] A. García-Miranda Ferrari, C.W. Foster, P.J. Kelly, D.A.C. Brownson, C.E. Banks, Determination of the electrochemical area of screen-printed electrochemical sensing platforms, Biosensors 8 (2018) 53, https://doi.org/10.3390/bios8020053.
[48] S.J. Konopka, B. McDuffie, Diffusion coefficients of ferri- and ferrocyanide ions in aqueous media, using twin-electrode thin-layer electrochemistry, Anal. Chem 42 (1970) 1741–1746, https://doi.org/10.1021/ac50160a042.
[49] M.A. Khan, R.D. Crapnell, E. Bernalte, B.L. Riehl, S.J. Rowley-Neale, C.E. Banks, Exploring the use of different carbon materials within additive manufactured electrodes: the sensing of carbendazim, Electroanalysis 37 (2025) e70016, https://doi.org/10.1002/elan.70016.
[50] R. Agarwal, The Nicholson method of determination of the standard rate constant of a quasireversible redox couple employing cyclic voltammetry: everything one needs to know!, ACS Electrochem. 1 (2025) 1885–1894, https://doi.org/10.1021/acselectrochem.5c00214.
[51] M. Zamani, V. Yang, L. Maziashvili, G. Fan, C.M. Klapperich, A.L. Furst, Surface requirements for optimal biosensing with disposable gold electrodes, ACS Meas. Sci. Au 2 (2022) 91–95, https://doi.org/10.1021/acsmeasuresciau.1c00042.
[52] A.D. Robles, S.N. Vettorelo, M. Gerpe, F. Garay, The electrochemical reaction mechanism of arsenic on gold analyzed by anodic stripping square-wave voltammetry, Electrochim. Acta 227 (2017) 447–454, https://doi.org/10.1016/j.electacta.2016.12.181.
[53] C. Jeyabharathi, P. Ahrens, U. Hasse, F. Scholz, Identification of low-index crystal planes of polycrystalline gold on the basis of electrochemical oxide layer formation, J. Solid State Electrochem 20 (2016) 3025–3031, https://doi.org/10.1007/s10008-016-3228-1.
[54] M. Drozd, P. Ivanova, K. Tokarska, K. Żukowski, A. Kramarska, A. Nowiński, E. Kobylska, M. Pietrzak, Z. Brzózka, E. Malinowska, Versatile and easily designable polyester-laser toner interfaces for site-oriented adsorption of antibodies, Int. J. Mol. Sci 23 (2022) 3771, https://doi.org/10.3390/ijms23073771.
[55] E. Piccin, D. Ferraro, P. Sartori, E. Chiarello, M. Pierno, G. Mistura, Generation of water-in-oil and oil-in-water microdroplets in polyester-toner microfluidic devices, Sens. Actuator B-Chem 196 (2014) 525–531, https://doi.org/10.1016/j.snb.2014.02.042.
[56] A.-L. Liu, F.-Y. He, Y.-L. Hu, X.-H. Xia, Plastified poly(ethylene terephthalate) (PET)-toner microfluidic chip by direct-printing integrated with electrochemical detection for pharmaceutical analysis, Talanta 68 (2006) 1303–1308, https://doi.org/10.1016/j.talanta.2005.07.043.
[57] L. Trnkova, X. Li, M. Vojs, P. Michniak, M. Marton, O. Matvieiev, J. Čechal, V. Stepanova, Surface electron transfer enhanced by molecular oxygen: droplet and bulk mode experiments on boron-doped diamond electrodes, J. Electroanal. Chem 995 (2025) 119329, https://doi.org/10.1016/j.jelechem.2025.119329.
[58] N. Dossi, R. Toniolo, F. Terzi, F. Impellizzieri, G. Bontempelli, Pencil leads doped with electrochemically deposited Ag and AgCl for drawing reference electrodes on paper-based electrochemical devices, Electrochim. Acta 146 (2014) 518–524, https://doi.org/10.1016/j.electacta.2014.09.049.
[59] O.A.S. Rafea, A.M. Abdel-Aziz, M.A. Sayed, R.M. Abdelhameed, I.H.A. Badr, Enhanced simultaneous voltammetric detection of lead, copper, and mercury using a MIL-101(Cr)-(COOH)2@MWCNTs modified glassy carbon electrode, Anal. Chim. Acta 1338 (2025) 343600, https://doi.org/10.1016/j.aca.2024.343600.
[60] E.M. Richter, M.A. Augelli, S. Magarotto, L. Angnes, Compact disks, a new source for gold electrodes. Application to the quantification of copper by PSA, Electroanalysis 13 (2001) 760–764, https://doi.org/10.1002/1521-4109(200105)13:8/9≤760::AID-ELAN760≥3.0.CO;2-N.
[61] S. Laschi, I. Palchetti, M. Mascini, Gold-based screen-printed sensor for detection of trace lead, Sens. Actuator B-Chem 114 (2006) 460–465, https://doi.org/10.1016/j.snb.2005.05.028.
[62] M.F. Md Noh, I.E. Tothill, Development and characterisation of disposable gold electrodes, and their use for lead(II) analysis, Anal. Bioanal. Chem 386 (2006) 2095–2106, https://doi.org/10.1007/s00216-006-0904-5.
[63] E.S. Almeida, E.M. Richter, R.A.A. Muñoz, On-site fuel electroanalysis: determination of lead, copper and mercury in fuel bioethanol by anodic stripping voltammetry using screen-printed gold electrodes, Anal. Chim. Acta 837 (2014) 38–43, https://doi.org/10.1016/j.aca.2014.05.031.
[64] M.L.S. Vasconcellos, D.P. Rocha, S.V.F. Castro, L.R.G. Silva, R.A.A. Muñoz, M.B.J. G. Freitas, R.Q. Ferreira, Electroanalytical method for determination of trace metals in struvite using electrochemically treated screen-printed gold electrodes, J. Braz. Chem. Soc 31 (2020) 1873–1882, https://doi.org/10.21577/0103-5053.20200081.

[65] F. Rueda-Holgado, E. Bernalte, M.R. Palomo-Marín, L. Calvo-Blázquez, F. Cereceda-Balic, E. Pinilla-Gil, Miniaturized voltammetric stripping on screen printed gold electrodes for field determination of copper in atmospheric deposition, Talanta 101 (2012) 435–439, https://doi.org/10.1016/j.talanta.2012.09.054.

[66] E. Bernalte, S. Arévalo, J. Pérez-Taborda, Jannis Wenk, P. Estrela, A. Avila, M. Di Lorenzo, Rapid and on-site simultaneous electrochemical detection of copper, lead and mercury in the Amazon river, Sens. Actuator B-Chem 307 (2020) 127620, https://doi.org/10.1016/j.snb.2019.127620.

[67] M. Abate, G. Bontempelli, N. Dossi, Gold leaf electrodes for UV/Vis spectroelectrochemical determination of ortho-diphenols in extra virgin olive oil, Talanta 284 (2025) 127215, https://doi.org/10.1016/j.talanta.2024.127215.